This article has been accepted for publication in a future issue of this journal, but has not been fully edited. Content may change prior to final publication. Citation information: DOI 10.1109/LAWP.2016.2565610, IEEE Antennas and Wireless Propagation Letters

Unidirectional Wideband 3-D Antenna for Human Head-Imaging Application

Md. Rokunuzzaman, Md. Samsuzzaman, St. Member IEEE and Mohammad Tariqul Islam, Sr., *Member, IEEE*

***Abstract*—A compact *3D* stacked patch antenna is presented for microwave head imaging application. Stacked patch technique is utilized to achieve unidirectional radiation pattern and folding technique is used to achieve resonance at lower frequency that are the requirements for imaging system. Shorting wall is introduced to minimize the overall antenna structure. The proposed antenna resonance frequency is *2.65–2.91 GHz* with an average gain of *6.6 dBi* at *2.7 GHz*. The dimension of the antenna is $25 \times 25 \times 10.5$ *mm*^{3}. The operating frequency of the proposed antenna is suitable for human brain imaging. The sensor characteristic of the proposed antenna is affiliated via connection with the imaging entity, miniaturized dimension and high radiation efficiency. Raster scanning is deployed to achieve the 2D image of the target phantom and it is shown that the proposed highly directional antenna can detect tumor inside the human brain phantom.**

***Index Terms*—Microwave imaging, Human head, three dimensional antenna, high gain, miniaturization.**

I. Introduction

MICROWAVE imaging technique is recently given higher priority due to its low cost, portability and side effect minimization nature compared to other existing solutions. One of the most important and sophisticated filed in imaging is human head-imaging (HHI).There are a number of brain diseases which if not detected at early stage, might end up resulting in premature death. The frequency specification for HHI is from 1-4 GHz [1]. In Microwave imaging, the antenna is the key element for connection between the head and the back end of the microwave imaging system. The dimension and radiation characteristics of the antenna control the overall microwave imaging performance greatly. To be portable and at the same time have all the characteristics desired by the microwave imaging system is a challenging task specifically when it comes to the most sensitive part of human body (head). As HHI frequency specification is at the low microwave frequency band, the dimension of the antenna needs to fulfill the minimum requirement [1]. This specific band for HHI is used to have a reasonable compromise between the resultant microwave image resolution and the penetration of the microwave signal inside the head. Another reason behind the low microwave frequency selection is to limit the human head exposing to the radiation power well within acceptable range [2]. One important characteristic for any imaging antenna is high directivity which makes the positioning of the imaging process much easier and the processing of the image becomes simpler. With a highly directive antenna, the precision of the traumatic tissue detection grows to be much effective. To attain high directivity and gain in the antennas of microwave imaging system, a few efforts has been made recently [3-5]. Dielectric resonator antenna (DRA) with 3-D structure is reported to have a wide bandwidth [3]. However, the directivity of the antenna is not much suitable for the HHI. Also in [6] and [7], the band of interest is covered for HHI. Nonetheless, in these cases the gain of the antenna is 4 dBi and 2.5 dBi respectively at the operating range and the radiation pattern is not highly directive. To make the microwave imaging system portable, the miniaturization of the antenna dimension is also necessary [4, 6]. A new approach is required to increase the gain, directivity, as well as the miniaturization of the antenna dimension to meet the portability specification.

In this letter, a 3-D structure is proposed with the heterogeneous combination of conventional 3-D antenna design techniques and post optimization. A parallel structure is attached with the feeding structure of the antenna to achieve resonance at lower frequency. Then the structure folded using parametric studies to achieve miniaturization and low frequency operation. To reduce the effect of folding, a square shaped patch is introduced at the end of the folded structure which also aids to achieve high gain. Stacked patch is used to achieve unidirectional radiation pattern throughout the operating frequency. The final structure achieves a constant gain of 6.6 dBi throughout the frequency ranging from *2.65–2.91* GHz. The proposed 3-D structure is compact in size and highly unidirectional towards the normal of the xy-plane.

II. Design of the 3-D Structure

Coaxial probe feeding reduces the spurious radiation occurred by other feeding method; hence it is applied to the design structure. Due to high *Q* leakage of the resonator, coaxial probing system depicts a restricted resonance bandwidth. Also, with the increment in probe length, the inductance along the line of probe becomes more effective which results in narrow bandwidth. By decreasing the length of the probe, this inductance can be controlled. The lower microwave frequency range highly depends on the overall dimension of the radiating structure. At the same time, the miniaturization of the antenna

Md. Rokunuzzaman is at the School of Engineering, RMIT University, Melbourne, Victoria 3001, Australia. (E-mail: robelhk@yahoo.com).
Md. Samsuzzaman is at the faculty of CSE, Patuakhali Science and Technology University, Bangladesh. (E-mail: samsuzzaman@siswa.ukm.edu.my).
Mohammad Tariqul Islam is at the department of Electrical, Electronic and Systems Engineering, Universiti Kebangsaan Malaysia, Bangi 43600, Malaysia (e-mail: tariqul@ukm.edu.my).

This article has been accepted for publication in a future issue of this journal, but has not been fully edited. Content may change prior to final publication. Citation information: DOI 10.1109/LAWP.2016.2565610, IEEE Antennas and Wireless Propagation Letters

is limited by the frequency it is operating on. To achieve low frequency and miniaturization effectively, folding technique must be used. Fig. 1 exhibits the geometry of the antenna. The proposed structure is built at the center of a square shaped ground plane. To reduce the overall size of the antenna, a shorting wall is extended until the ground plane of the antenna [8, 9] which makes the antenna to resonate at a lower frequency. The width of the shorting wall is kept same as the radiating plane of the structure for simplicity. The lower patch is U-shaped and directly connected with the coaxial probe. The placement of the coaxial probe is crucial relative to the lower patch and optimized to achieve desired performance (not shown for brevity). To achieve decreased inductance at the operating frequency, the height of the probe is minimized.

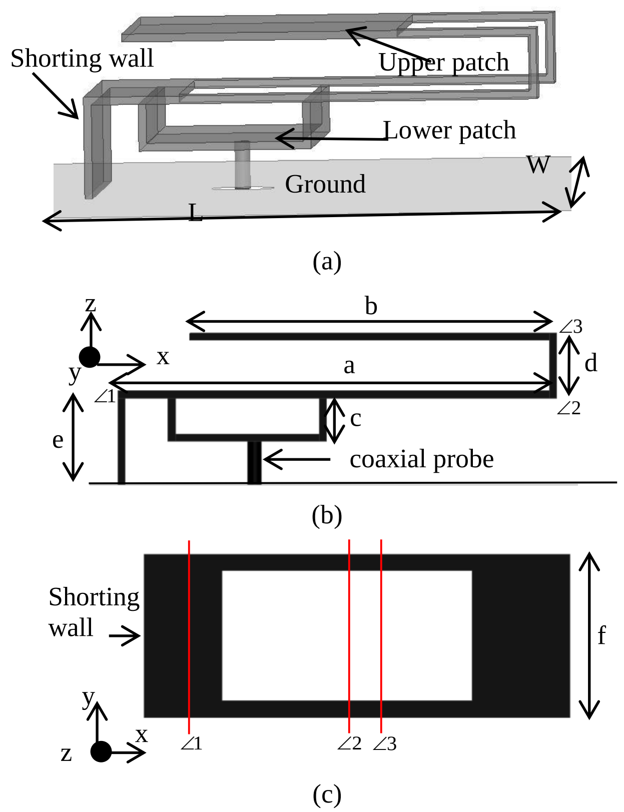

Fig. 1. Configuration of the proposed 3-D structure, (a) 3-D view, (b) side view, (c) 2-D copper sheet for bended structure construction.

TABLE I

STRUCTURE DESIGN PARAMETERS (in millimeters)

a	25	c	3	e	6	L	80
b	20	d	4.5	f	25	W	80

The overall length of the patch sitting on the lower patch is $x = 55.5$ *mm* as shown in Fig. 1 (b). The resonance frequency for this dimension can be roughly calculated using the equation described in [10]:

$$f_r = \frac{c}{\left[x\sqrt{2(\varepsilon_r + 1)}\right]} \quad (1)$$

Here, c is the speed of light, f_r is the center frequency of the resonance band, ε_r is the relative permittivity of the antenna material and x is the overall length of the upper patch. The shorting wall and the radiating antenna are constructed using 0.2 mm thick copper sheets. Air is the substrate for the whole antenna structure; hence, the structure over the plain copper ground plane is entirely supported by the coaxial probe and the shorting pin. The structure has an overall height of *10.5 mm* (from the ground plane until the upper patch) and the probe height is set to be *3 mm* to achieve miniaturized dimension. Fig. 1 (b) depicts the cross section of the structure. The antenna is composed of a shorting wall, lower patch (U-shaped) and an upper patch. A simplified process to construct the antenna structure using a 2D copper sheet as shown in Fig. 1 (c). Bending the points as shown in the picture, will result in the shorting wall included with the upper patch. Then the upper patch needs to be set over the corners of the U-shaped lower patch. The structure is symmetrical at the xz-plane. The points of bending are kept at a distance from the feeding point to minimize the disturbance of the current concentration [11, 12].The upper patch is rectangle shaped, held by the bended extensions from the lower patch. Through parametric studies, the gap between the patches is optimized to be *d*. The height of the square patch from the ground is *e+d*. The proportion of coupling between the two patches can be used to tune the resonance frequency of the structure. To achieve higher gain, both patches are stacked at a position to achieve high directivity normal to the ground plane of the antenna. With the change in the size of the rectangular patch, the radiation pattern of the antenna changes gradually. The rectangular patch actively couples with the U-shaped patch hence passively coupling with the coaxial probe beneath the lower patch, the reactance decreases at the feeding point with the increment in resistance of the input impedance. Through parametric studies, it can be observed that "*a*" plays an important role in tuning the resonance frequency of the antenna. The coupling effect between the U-shaped patch and the lower part (before bending) of the rectangular patch cancels the reactance in between which results in increment in the real impedance.

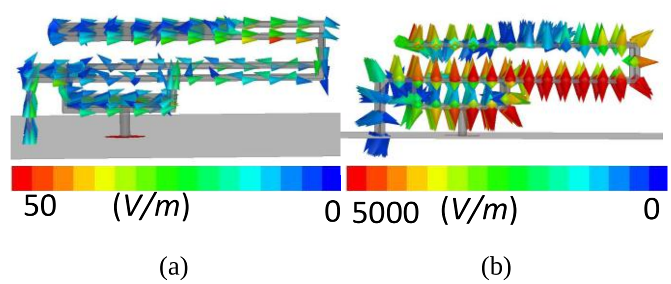

Fig. 2. Cross section view of the antenna (a) surface current distribution and (b) vector E-field at 2.7 GHz frequency

Fig. 2 depicts the (a) surface current and vector E-field distribution of the proposed antenna. From Fig. 2 (a), it can be observed that the direction of current flow is heading towards the main beam point of the radiation pattern and maximum current density is occurring at the edge of the stacked patches connection point. Hence direct connection between the patches is crucial for the design. Moreover, the current flow direction from the shorting wall towards the main patch confirms the mechanism of the wall for the particular frequency. Fig. 2 (b) shows the vector E-field where the field is stronger over the

This article has been accepted for publication in a future issue of this journal, but has not been fully edited. Content may change prior to final publication. Citation information: DOI 10.1109/LAWP.2016.2565610, IEEE Antennas and Wireless Propagation Letters

feeding point of the stacked patches, hence a high directivity can be observed toward the +z direction. At the edge of the patch connection, the amount of power is almost identical for the two patches and cancelling each other. However, due to the comparatively strong E-field at the back (-z direction) of the 1st patch, the back lobe of the radiation pattern results in at 2.7 GHz.

III. Results and Discussion

a. Antenna Characteristics

The optimum design with the dimensions listed in Table I was fabricated and tested. The antenna was first built in three planar fragments, then bending one part and soldered together. The simulated and measured reflection coefficients (S_{11}) of the antenna are presented in Fig. 3(a). The antenna has a measured S_{11} below -10 dB at 2.65–2.91 GHz. The antenna gain was simulated and measured in Satimo near field anechoic chamber (Star Lab) along the main radiation (direction). It can be seen from Fig. 3(b) that the antenna has a high gain with a peak value of 6.60 dBi. To ensure that antenna radiates most of its accepted power in the forward direction, its far-field radiation patterns were simulated and measured, and the results at 2.7 GHz frequency is presented in Fig. 3(c). The antenna shows a unidirectional radiation pattern with a peak measured front-to-back ratio (FBR) (direction) of 19 dB which is greater than [4] [13] . The antenna has negligible cross polarization, which is not presented for brevity. The overall simulated and measured performances of the antenna are in reasonable agreement. The small discrepancies at certain frequencies are due to the fabrication errors from the imperfect manual building of the 3-D antenna structure. Figure 3(d) also illustrates the E-filed distribution of the used phantom at 2.70 GHz.

b. Microwave Imaging setup and measurement

The proposed antenna is tested for the detection of abnormal tissue in brain by utilizing microwave imaging technology in computational environment. The set-up for the anomaly tissue detection begins with detecting element, which is the proposed antenna, and the model of human brain tissue along with the bone and other layers involved. A symmetrical brain phantom is developed with the characteristics shown in Table 2 [14-16]. Two antennas are used to scan the brain structure where one is the transmitter and the other one is the receiver antenna. The signal passes through the brain model while antennas are transmitting and receiving. The antennas are moved at plane symmetry to each other and moved within the surface of the phantom to achieve 2-D scanning of the whole brain. As the brain is covered by the hardest structure of the human body, it is not possible to compress or reshape the brain structure. Fig. 4 shows the brain phantom with the necessary properties that are considered here. Both the antennas are kept at 20 mm distance from the brain. While scanning the breast of human body [17], the antennas do not need to be as highly directional compared to when scanning a brain. This is because breast has no bone structure whereas; brain tissue is covered by the thick layer of compact (cortical) bone [15] and microwave signal can be easily reflected and refracted from this dense bone structure.

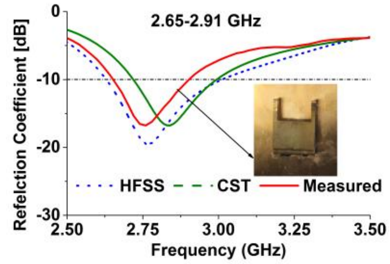

(a)

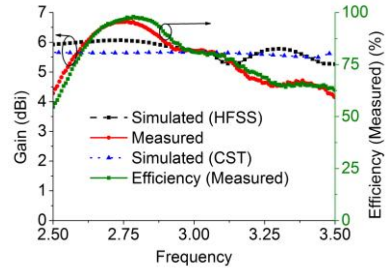

(b)

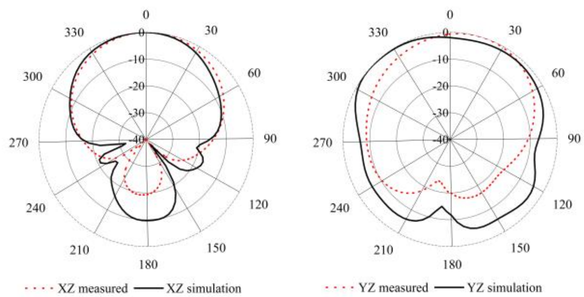

(c)

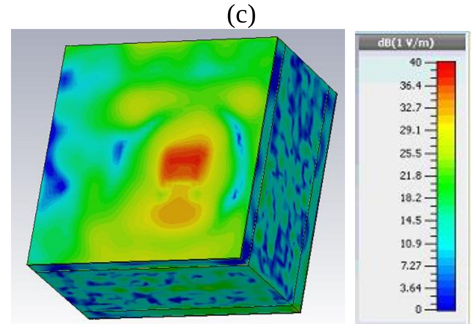

(d)

Fig. 3. Simulated versus measured (a) reflection coefficient, (b) gain, efficiency (c) radiation pattern and (d) E field distribution at 2.7 GHz.

To overcome this challenge, the proposed antenna is made highly directional with ignorable amount of back-lobe power. This imaging setup bares the advantages of (i) no external coupling liquid, (ii) direct coupling between antennas through the tissue (high near field directivity), and (iii) the image processing is simple. To get calibrated sensing response from the setup, the response between antennas without the phantom, $S_{21}^{background}$ measurement is taken at yz-plane (no scattering is present and considering the background medium) which is the difference from the ideal case to the practical measurement environment. Later, this measurement $|S_{21}^{background}|$ is deducted from the measurement $|S_{21}^{measurement}|$ which includes the brain phantom in the middle of the propagation way, where all the measurements are taken at the yz-plane. With the background

This article has been accepted for publication in a future issue of this journal, but has not been fully edited. Content may change prior to final publication. Citation information: DOI 10.1109/LAWP.2016.2565610, IEEE Antennas and Wireless Propagation Letters

portion removed from the measurement response, the output of the calculation shown in (2) can be expressed as calibrated output $|S_{21}^{calibrated}|$ [18]:

$$S_{21}^{calibrated} = S_{21}^{measurement} - S_{21}^{background} \qquad (2)$$

In Fig. 4, the human brain phantom is constructed using the parameters given in Table 2. The experiment is performed on a healthy and unhealthy (malignant) brain. The S_{21} parameter is acquired in an area of 140 mm ×140 mm where the sampling rate is 5 mm. Fig. 5(a)–(b) show the images obtained from $|S_{21}^{calibrated}|$ at 2.7 GHz. The actual location of the tumor is portrayed by red color sensitivity. From these figure, it can be observed that the location of the tumor can be identified with high resolution and sensitivity processing in the malignant brain with red color , whereas the healthy brain has no significant scattered with same color (blue) scale. The overall performance of the obtained results confirm the suitability of the antenna in the microwave imaging application.

TABLE II

DIELECTRIC PROPERTIES OF THE BRAIN PHANTOM (Ɛ)

Material	Dielectric Constant (Ɛ)	Thickness (mm)	S m^{-1}
Skin	38	1	1.61
Grey matter	45	60	2.03
Skull	14.9	10	0.913
Tumor	67	5 (sphere radius)	2.30

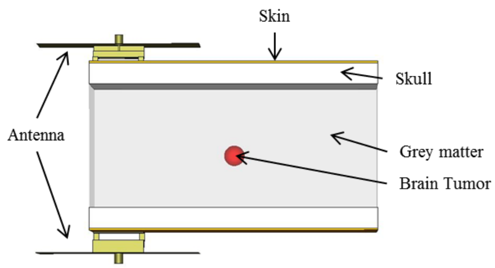

Fig. 4. Microwave imaging setup to detect tumor inside human brain phantom.

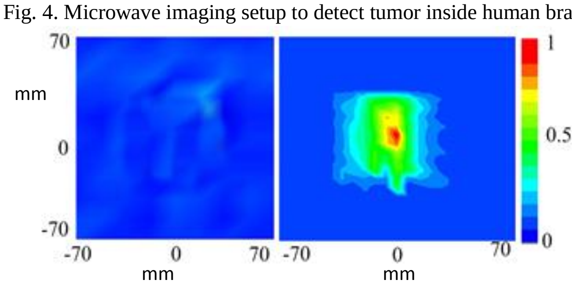

(a) (b)

Fig. 5. Imaging results for (a) healthy brain (b) brain with malignant tumor

IV. CONCLUSION

In this paper, a 3-D antenna is presented that utilizes stacked patch with folding technique for miniaturization of the antenna dimension. The antenna is compact in size with a dimension of 0.23λ × 0.23λ × 0.09λ. The antenna has a high directivity throughout the operating frequency while the size is kept compact. A shorting wall is used for the antenna to resonate at a lower frequency with high gain. The radiation characteristic of the antenna is appropriate for highly directive application. The proposed unidirectional antenna has a pick front to back ratio of 19 dB. The average gain of the antenna is 6.6 dBi in the achieved operating band 2.65 GHz to 2.91 GHz. This characteristic makes the antenna a perfect candidate for microwave head imaging application. The performance of the antenna is evaluated by successfully detected a tumor in a human brain phantom through raster scanning imaging method of a 2D plane. Air substrate and *0.2 mm* thick copper sheet is utilized to construct the antenna.

REFERENCES

[1] B. J. Mohammed, A. M. Abbosh, S. Mustafa, and D. Ireland, "Microwave system for head imaging," *Instrumentation and Measurement, IEEE Transactions on,* vol. 63, pp. 117-123, 2014.

[2] o. N.-I. R. H. IEEE Standards Coordinating Committee 28, *IEEE Standard for Safety Levels with Respect to Human Exposure to Radio Frequency Electromagnetic Fields, 3kHz to 300 GHz*: Institute of Electrical and Electonics Engineers, Incorporated, 1992.

[3] A. Sabouni and A. Kishk, "Dual-polarized, broadside, thin dielectric resonator antenna for microwave imaging," *Antennas and Wireless Propagation Letters, IEEE,* vol. 12, pp. 380-383, 2013.

[4] A. T. Mobashsher, A. M. Abbosh, and Y. Wang, "Microwave system to detect traumatic brain injuries using compact unidirectional antenna and wideband transceiver with verification on realistic head phantom," *Microwave Theory and Techniques, IEEE Transactions on,* vol. 62, pp. 1826-1836, 2014.

[5] X. Li, M. Jalilvand, Y. L. Sit, and T. Zwick, "A compact double-layer on-body matched bowtie antenna for medical diagnosis," *Antennas and Propagation, IEEE Transactions on,* vol. 62, pp. 1808-1816, 2014.

[6] A. T. Mobashsher and A. Abbosh, "Slot-loaded folded dipole antenna with wideband and unidirectional performance for L-band applications," *Antennas and Wireless Propagation Letters, IEEE,* vol. 13, pp. 798-801, 2014.

[7] S. Ahdi Rezaeieh and A. Zamani, "3-D Wideband Antenna for Head-Imaging System with Performance Verification in Brain Tumor Detection," *Antennas and Wireless Propagation Letters, IEEE,* vol. 14, pp. 910-914, 2015.

[8] C. Chiu, H. Wong, and C. Chan, "Study of small wideband folded-patch-feed antennas," *IET Microwaves, Antennas & Propagation,* vol. 1, pp. 501-505, 2007.

[9] T. Taga and K. Tsunekawa, "Performance Analysis of a Built-In Planar Inverted F Antenna for 800 MHz Band Portable Radio Units," *IEEE Journal on Selected Areas in Communications,* vol. 5, pp. 921-929, 1987.

[10] W.-L. Chen, G.-M. Wang, and C.-X. Zhang, "Bandwidth enhancement of a microstrip-line-fed printed wide-slot antenna with a fractal-shaped slot," *Antennas and Propagation, IEEE Transactions on,* vol. 57, pp. 2176-2179, 2009.

[11] S. Ahdi Rezaeieh, A. Abbosh, and Y. Wang, "Wideband unidirectional antenna of folded structure in microwave system for early detection of congestive heart failure," *Antennas and Propagation, IEEE Transactions on,* vol. 62, pp. 5375-5381, 2014.

[12] C. M. Kruesi, R. J. Vyas, and M. M. Tentzeris, "Design and development of a novel 3-D cubic antenna for wireless sensor networks (WSNs) and RFID applications," *Antennas and Propagation, IEEE Transactions on,* vol. 57, pp. 3293-3299, 2009.

[13] S. Ahdi Rezaeieh, A. Zamani, and A. Abbosh, "3-D Wideband Antenna for Head-Imaging System with Performance Verification in Brain Tumor Detection," *IEEE Antennas and Wireless Propagation Letters,* vol. 14, pp. 910-914, 2015.

[14] K. Foster, J. Schepps, R. Stoy, and H. P. Schwan, "Dielectric properties of brain tissue between 0.01 and 10 GHz," *Physics in medicine and biology,* vol. 24, p. 1177, 1979.

[15] S. Gabriel, R. Lau, and C. Gabriel, "The dielectric properties of biological tissues: II. Measurements in the frequency range 10 Hz to 20 GHz," *Physics in medicine and biology,* vol. 41, p. 2251, 1996.

[16] A. Peyman, S. Holden, S. Watts, R. Perrott, and C. Gabriel, "Dielectric properties of porcine cerebrospinal tissues at microwave frequencies: in vivo, in vitro and systematic variation with age," *Physics in medicine and biology,* vol. 52, p. 2229, 2007.

[17] M. Jalilvand, X. Li, L. Zwirello, and T. Zwick, "Ultra wideband compact near-field imaging system for breast cancer detection," *IET Microwaves, Antennas & Propagation,* 2015.

[18] R. K. Amineh, M. Ravan, A. Trehan, and N. K. Nikolova, "Near-field microwave imaging based on aperture raster scanning with TEM horn antennas," *Antennas and Propagation, IEEE Transactions on,* vol. 59, pp. 928-940, 2011.